Nuclear-structure aspects of nonanalog pion double charge exchange

R. Gilman and H. T. Fortune
University of Pennsylvania, Philadelphia, Pennsylvania 19104

Mikkel B. Johnson
Los Alamos National Laboratory, Los Alamos, New Mexico 87545

E. R. Siciliano*
University of Georgia, Athens, Georgia 30602

H. Toki
Tokyo Metropolitan University, Tokyo 158, Japan

A. Wirzba†
State University of New York at Stony Brook, Stony Brook, New York 11794

B. Alex Brown
Michigan State University, East Lansing, Michigan 48824
(Received 22 May 1986)

The sensitivity of pion double charge exchange to nuclear structure in the shell model is examined. We consider the nonanalog ground-state to ground-state ($T=0$ to $T=2$) transitions on a variety of nuclear targets. The reaction model, which assumes that double charge exchange is driven by a $\pi+\rho$-meson–mediated, Δ_{33}-nucleon interaction, reproduces the energy dependence and shape of the empirical cross section for all the (π^+,π^-) transitions examined. The magnitude of the cross section is particularly sensitive to collectivity in the nuclear wave functions. All parameters of the model, with the exception of the range of the meson-Δ_{33} form factor, are fixed by theoretical arguments. The form factor is then determined by normalizing to the $^{16}O(\pi^+,\pi^-)^{16}Ne$ cross section. Predictions are made for a variety of other low-lying 0^+ transitions.

In a recent paper,[1] we studied the nonanalog pion double-charge-exchange (DCX) reaction $^{16}O(\pi^+,\pi^-)^{16}Ne$(g.s.) based on the nonsequential delta-nucleon interaction (DINT) mechanism of Fig. 1, in which the Δ_{33}-nucleon interaction is mediated by $\pi+\rho$ meson exchange. Those calculations, which were an extension of earlier work,[2] provided a simple explanation of two of the regular features of nonanalog DCX: (1) the shape of the angular distribution, and (2) the peaking of the cross section near 160 MeV. The former feature is determined by the size of the nucleus, as in any strong absorption picture. This result might be considered surprising because there is no such simple relationship for analog DCX.[3] The second feature is a manifestation of a strong energy dependence of the DINT reaction model arising from the succession of Δ_{33} excitations on the *same* nucleon. The cross section arising from sequential charge exchange on two *different* nucleons can also contribute and will be the subject of future work.[4] A first attempt to calculate this process gave the wrong energy dependence.[5]

In this paper we examine whether the A dependence of pion DCX ground-state to ground-state ($T=0$ to $T=2$) transitions can be understood from the theory of Refs. 1 and 2. We compare to all measured (π^+,π^-) excitation functions and angular distributions for the targets ^{12}C, ^{16}O, ^{24}Mg, ^{28}Si, ^{32}S, ^{40}Ca, ^{44}Ca, and ^{56}Fe (in the latter two cases, the initial state is $T=2$ and the final state $T=0$).

Realistic wave functions were obtained with model-space interaction combinations used in recent literature. These are summarized in Table I. For $A=24$, 28, and 32 within the assumed model space it was necessary to make additional truncations which, however, are not severe. For $A=56$, we assume a 2p2h configuration relative to a closed $0f_{7/2}$ shell. The wave functions and two-body transition densities were obtained with the shell-model code OXBASH,[6] and the two-body transition densities are as defined in Ref. 7. At present, restrictions in the reaction calculations allow pairs of nucleons coupled only to $J=0$ to participate.

In Ref. 1 we described $^{16}O(\pi^+,\pi^-)^{16}Ne$ as a simple $(p_{1/2})^2\rightarrow(d_{5/2})^2$ transition. It is clear from Table I that the actual wave function is more complicated: None of the transitions shown in Table I can be represented by a simple excitation between two orbitals. Because the angle and energy dependences of cross sections are indicative of the reaction mechanism, the choice of more realistic wave functions will not change the conclusions of Ref. 1. However, the overall magnitude of the cross section and its variation from nucleus to nucleus will be affected by the nuclear structure.

The model of the Δ_{33}-nucleon force was explained earlier in Ref. 2, to which the reader is referred for details.

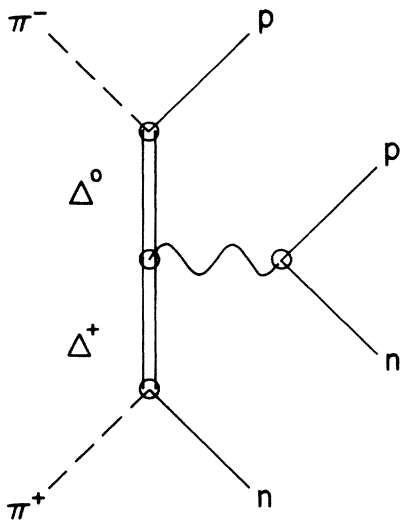

FIG. 1. A Feynman amplitude showing the DINT process considered in this paper. The interaction between the Δ_{33} and nucleon is assumed to occur through $\pi+\rho$ meson exchange, as discussed in the text. The cross section is obtained using realistic wave functions for the pion and nucleus.

The meson-Δ_{33} coupling constants are related to empirical determinations of meson-nucleon coupling constants by SU(2)×SU(2) quark-model arguments. The mass of the ρ meson and its coupling strength are chosen to account for the resonant plus two-pion continuum parts of the $J^\pi=1^-$ NN→$\pi\pi$ helicity amplitude. Short-range repulsive correlations between the nucleon and Δ_{33} are approximated by an appropriate cutoff in the radial integrals. Unlike the meson-nucleon case, the meson-Δ_{33} form factors are not known empirically at the present time, and we determine them by normalizing to the $^{16}O(\pi^+,\pi^-)^{16}Ne$ datum at 165 MeV and 5°.

We have considered several variations of the above model. Unless stated otherwise, the numerical results shown in the figures and tables are based on a simple version (model I) of the theory that closely follows Refs. 1 and 2: The form factors have the simple shape $v(p)=(p^2/\Lambda^2+1)^{-1}$, the cutoff in the radial integrals is a simple step function at 0.5 fm, and the optical potential determining the initial and final pion distorted waves is linear in the density and related in the usual way to the pion-nucleon phase shifts. The coupling constant $f_{\pi N\Delta}$ is related to $f_{\pi NN}$ by $f^2_{\pi N\Delta}/f^2_{\pi NN}=4.5$ and $\Lambda_\rho=\Lambda_\pi=4.6$ fm^{-1}. We take the $\Lambda_{\pi,\rho}$ to be the same for the Δ_{33} and the nucleon. Note that the values of Λ_π and Λ_ρ are substantially changed from those in Refs. 1 and 2 when realistic wave functions are used in order to reproduce the magnitude of the ^{16}O data. In model I of this paper, we take $m_\rho=650$ MeV and $C_\rho=(f_\rho m_\pi/f_\pi m_\rho)^2=2$. Later we indicate how the results change when we make a few more realistic assumptions.

The results based on realistic wave functions are compared to those obtained from the simplest configurations in Table II. In general the realistic choice results in a

TABLE I. Microscopic transition amplitudes from shell-model calculations.

Nuclei	Model space	Interaction	Transition[f]
$^{12}C\rightarrow{}^{12}O$	$(0p_{3/2},0p_{1/2})^8$	(6−16)2BME[a]	$0.335p^2\rightarrow p^2+0.982p^2\rightarrow p'^2+0.426p'^2\rightarrow p'^2$
$^{16}O\rightarrow{}^{16}Ne$	$(0p_{1/2},0d_{5/2},1s_{1/2})^4$	*F-pds*[b]	$0.200p'^2\rightarrow p'^2-0.777p'^2\rightarrow d^2-0.616p'^2\rightarrow s^2$ $+0.248d^2\rightarrow d^2+0.272d^2\rightarrow s^2+0.045s^2\rightarrow s^2$
$^{24}Mg\rightarrow{}^{24}Si$	$(0d_{5/2})^{(4-8)}$ $(1s_{1/2},0d_{3/2})^{(0-4)}$	Wildenthal[c]	$0.067d'^2\rightarrow d'^2+0.402d'^2\rightarrow d^2+0.138d'^2\rightarrow s^2$ $+0.660d^2\rightarrow d^2+0.401d^2\rightarrow s^2+0.065s^2\rightarrow s^2$
$^{28}Si\rightarrow{}^{28}S$	$(0d_{5/2})^{(8-12)}$ $(1s_{1/2},0d_{3/2})^{(0-4)}$	Wildenthal[c]	$0.145d'^2\rightarrow d'^2+0.528d'^2\rightarrow d^2+0.283d'^2\rightarrow s^2$ $+0.286d^2\rightarrow d^2+0.561d^2\rightarrow s^2+0.132s^2\rightarrow s^2$
$^{32}S\rightarrow{}^{32}Ar$	$(0d_{5/2})^{(8-12)}$ $(1s_{1/2},0d_{3/2})^{(0-4)}$	Wildenthal[c]	$0.357d'^2\rightarrow d'^2+0.346d'^2\rightarrow d^2+0.785d'^2\rightarrow s^2$ $+0.089d^2\rightarrow d^2+0.316d^2\rightarrow s^2+0.212s^2\rightarrow s^2$
$^{40}Ca\rightarrow{}^{40}Ti$	$(0d_{3/2},0f_{7/2})^8$	SAS[d]	$-0.326d'^2\rightarrow d'^2+1.099d'^2\rightarrow f^2-0.497f^2\rightarrow f^2$
$^{44}Ca\rightarrow{}^{44}Ti$	$(0f_{7/2},1p_{3/2},0f_{5/2},1p_{1/2})^4$	HG[e]	$0.780f^2\rightarrow f^2+0.439f^2\rightarrow p^2+0.270f^2\rightarrow f'^2$ $+0.216f^2+p'^2+0.061p^2\rightarrow p^2+0.076p^2\rightarrow f'^2$ $+0.061p^2\rightarrow p'^2+0.023f'^2\rightarrow f'^2+0.037f'^2\rightarrow p'^2$ $+0.015p'^2\rightarrow p'^2$
$^{56}Fe\rightarrow{}^{56}Ni$	$(0f_{7/2})^{(14-16)}$ $(1p_{3/2},0f_{5/2},1p_{1/2})^{(0-2)}$	HG[e]	$0.670f^2\rightarrow p^2+0.413f^2\rightarrow f'^2+0.297f^2\rightarrow p'^2$

[a]From Table 6 in Ref. 8.
[b]From Table I in Ref. 9.
[c]From Table 1 in Ref. 10.
[d]See Ref. 11.
[e]From Table 1c in Ref. 12. For the matrix elements that do not appear in this table, we use the MSDI interaction that is given in the first column in Table 1 in Ref. 13.
[f]Primed orbits are j lower, umprimed orbits are j higher. Also, a simplification arises because we take the magnitude of the transitions between two single particle states, 1→2 and 2→1, to be equal. This would not be the case if, for example, the oscillator parameter were chosen to be different for neutrons and protons.

TABLE II. Comparison of DCX cross sections based on the DINT mechanism at 164 MeV and $\theta=5°$ with simple and realistic wave functions.

Nuclei	Simple transition	σ_{simple} (nb/sr)	$\sigma_{\text{realistic}}$[a] (nb/sr)
$^{12}C\rightarrow{}^{12}O$	$p^2\rightarrow p'^2$	1127	1173
$^{16}O\rightarrow{}^{16}Ne$	$p'^2\rightarrow d^2$	519	485
$^{24}Mg\rightarrow{}^{24}Si$	$d^2\rightarrow d^2$	10.0	156
$^{28}Si\rightarrow{}^{28}S$	$d^2\rightarrow s^2$	50	289
$^{32}S\rightarrow{}^{32}Ar$	$s^2\rightarrow d'^2$	22	116
$^{40}Ca\rightarrow{}^{40}Ti$	$d'^2\rightarrow f^2$	128	102
$^{44}Ca\rightarrow{}^{44}Ti$	$f^2\rightarrow f^2$	8.5	57
$^{56}Fe\rightarrow{}^{56}Ni$	$f^2\rightarrow p^2$	9.0	53

[a]With transition amplitudes from Table I.

larger cross section and a smoother variation from nucleus to nucleus. The enhancement varies from a factor of unity near closed shells to a factor of 15 in the middle of the *sd* shell. For example, in $^{16}O(\pi^+,\pi^-)^{16}Ne$(g.s.) with the transition of Table I, the dominant component is the $p'^2\rightarrow d^2$ transition, which is approximately eight times larger in the DWIA amplitude than the $p^2\rightarrow s^2$, $d^2\rightarrow d^2$, and $d^2\rightarrow s^2$ transitions, and about 14 times larger than the $p^2\rightarrow p^2$ and $s^2\rightarrow s^2$ transitions. All of those contributions are in phase. The enhancement in the middle of the *s-d* shell shows that collectivity in the wave function can be very important in DCX. In transitions $(jl)\rightarrow(j'l')$ the cross sections are largest when $j=l\pm\frac{1}{2}$ and $j'=l'\mp\frac{1}{2}$.

Figure 2 displays the A dependence of the theory in comparison to the data at 165 MeV. The open squares are the results of model I described earlier. The theory has approximately the same A dependence as the data. This result strengthens the evidence that the delta-nucleon interaction of Ref. 2 is important for understanding the dynamics of pion double charge exchange.

How sensitive are our results to the choice of the single-particle basis? One has to be careful because the pion reactions are very sensitive to the tail of the wave function, where the harmonic oscillator functions begin to become unrealistic; the problem is especially severe for heavy nuclei. We have, in any case, tested the sensitivity to small variations in the harmonic-oscillator size parameter. Changes of a few percent in the value result in similarly-sized changes in the calculated cross sections. The values we used in our calculations were taken from electron-scattering parametrization (where available), or calculated from the ansatz

$$\hbar\omega=(45A^{-1/3}-25A^{-2/3})\text{ MeV}\ .$$

Figures 3 and 4 compare measured excitation functions and angular distributions on these nuclei with the theory. As expected, all excitation functions, both calculated (denoted by a solid line for model I) and measured, exhibit a peaked energy dependence. Perhaps the largest difference between theory and experiment is in the case of ^{56}Fe, for which the data are more strongly peaked at a lower energy than theory. All measured angular distributions

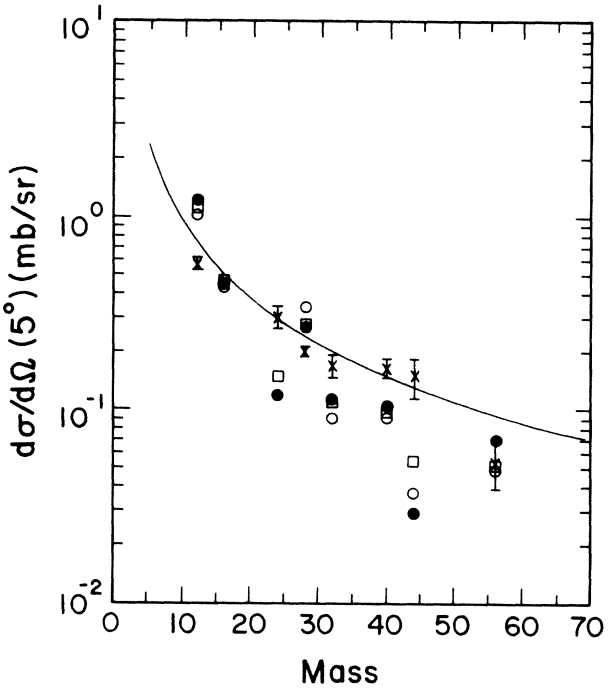

FIG. 2. The mass dependence of the nonanalog, ground-state to ground-state ($T=0$ to $T=2$) pion double-charge-exchange cross section at $\theta=5°$ and 165 MeV. The solid line indicates an $A^{-4/3}$ mass dependence. The data are (crosses with error bars) from Ref. 14. The open squares are model I, open circles model II, and solid circles model III, described in the text.

exhibit a first minimum that is consistent with the nuclear size, and are well represented by the calculations.

As stated earlier, the values of the π-meson and ρ-meson form factors have been determined from the $^{16}O(\pi^+,\pi^-)^{16}Ne$ data at 165 MeV. Next we want to show how these values change if we make slight changes in our assumptions. If we define the form factor in a more standard way[15] then

$$v(p)=\frac{\Lambda^2-m^2}{\Lambda^2+p^2}$$

for a meson of mass m. This coincides with our earlier choice in the limit that $\Lambda\rightarrow\infty$. We have also used a different determination of the 2π background to the ρ meson,[16] taking $m_\rho=644$ MeV and $(f_\rho m_\pi/f_\pi m_\rho)^2=2.6$. These are also slightly different from the values in Refs. 1 and 2. We take the nucleon-nucleon correlation function[17] to be

$$F(r)=1-j_0(m^*r)$$

with $m^*=783$ MeV. The open circles in Fig. 2 show the results of this (model II) calculation. Values for Λ are $\Lambda_\pi=5.10$ fm^{-1} and $\Lambda_\rho=5.95$ fm^{-1}. In determining these, we have kept the ratio Λ_ρ/Λ_π fixed at the values quoted in Ref. 15. Next, we make additional improvements involving the treatment of distorted waves in the DWIA calculation and the handling of the Q value in the process of Fig. 1. The solid circles (model III) show the

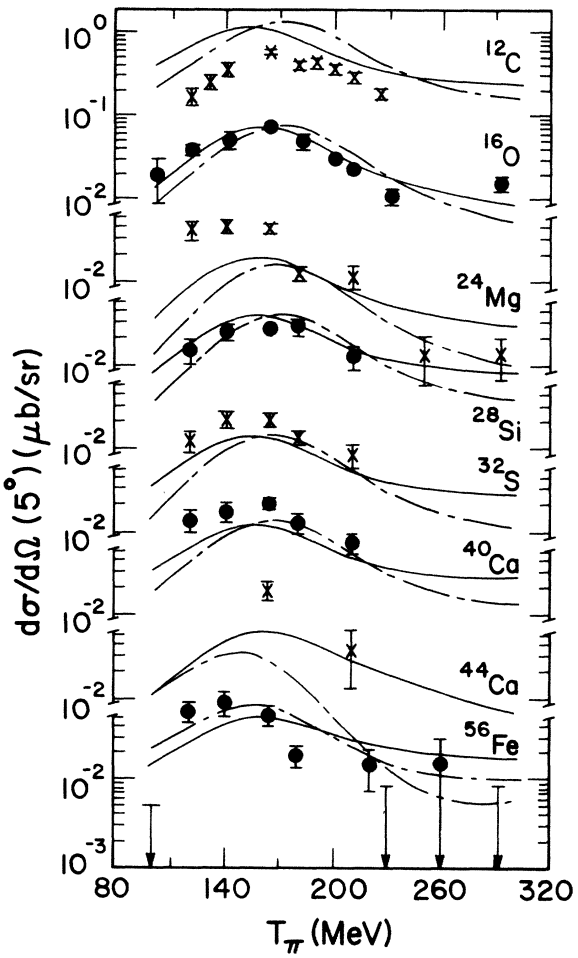

FIG. 3. The energy dependence of the 5° pion DCX cross section for nonanalog, ground-state to ground-state ($T=0$ to $T=2$) transitions. Data are from Ref. 14. The solid line is model I and the dash-dotted line model III, described in the text.

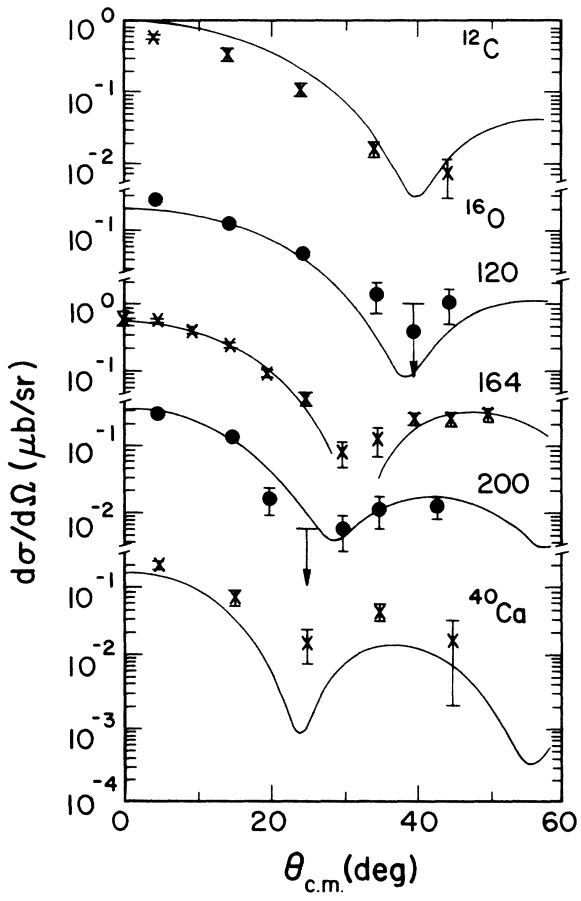

FIG. 4. The angle dependence of nonanalog, ground-state to ground-state ($T=0$ to $T=2$) pion DCX cross sections in model I. ^{16}O angular distributions are shown at three energies, indicated on the figure. The ^{12}C and ^{40}Ca angular distributions are for 164 MeV.

effect of these changes on model II. For this calculation of distorted waves we use the lowest order optical potential calculated from free pion-nucleon phase shifts, but we employ an energy shift[18] of 30 MeV which gives a uniformly improved description of elastic scattering. We shifted the energy in the two Δ isobar propagators in Fig. 1 by $Q/2$ to account roughly for the Q value in the reaction. When all these changes are made we find that the energy dependence of our cross sections is slightly improved (especially in the shift of the peak in Fig. 3 as A is changed), and the A dependence slightly deteriorates. The new values of Λ_π and Λ_ρ are $\Lambda_\pi=4.97$ fm^{-1}, $\Lambda_\rho=5.80$ fm^{-1}. These are smaller than the values found for $\Lambda_{\pi NN}$ and $\Lambda_{\rho NN}$ in the phenomenological studies of Ref. 15, corresponding to a somewhat larger Δ than nucleon.

Several predictions of transitions leading to residual 0^+ excited states in pion DCX are contrasted with residual ground-state cross sections in Table III. We again recognize the collective feature of DCX, especially for ^{16}O→^{16}Ne and ^{40}Ca→^{40}Ti, where the ground-state transitions totally dominate. The smaller excited-state cross sections (often smaller by an order of magnitude) would not have been observed experimentally. DCX experiments usually are limited to ~20% statistics for the ground state, which would result in only a few counts for these excited states. Most of the excited 0^+ states listed in Table III lie above the particle threshold and would acquire a width. On the other hand, for the case of the transitions from the unfilled ground states in ^{56}Fe→^{56}Ni and ^{32}Sc→^{32}Ar, there appear moderately strong transitions, at $E_x=3.75$ MeV and at $E_x=5.7$ MeV, respectively. It would be interesting to look for this transition experimentally.

A more general question is the contribution of DINT in DCX to non-0^+ states. Restrictions in our transition-density calculation currently prevent calculations of, for example, residual first-excited 2^+ states. Work is in progress to perform these calculations.

Our results are remarkable because of the simplicity of the underlying model, and they are important because they suggest that the pion double-charge-exchange reaction on well-understood nuclei provides a means of study-

TABLE III. Comparison of DCX cross sections for residual 0^+ states at 164 MeV and 5°.

Nuclei	Final state (MeV)	σ (nb/sr)
$^{16}O \rightarrow {}^{16}Ne$	g.s.	485
	2.60	75
	9.47	15
$^{32}Sc \rightarrow {}^{32}Ar$	g.s.	116
	4.97	10
	5.76	50
$^{40}Ca \rightarrow {}^{40}Ti$	g.s.	102
	3.92	19
	5.72	7
$^{56}Fe \rightarrow {}^{56}Ni$	g.s.	53
	3.09	16
	3.75	23

ing the Δ_{33}-nucleon interaction. However, the fact that this model is unable to account for analog transitions[2] remains to be explained. This failure may suggest that there is more to the Δ_{33}-nucleon interaction than the π- and ρ-exchange pieces discussed here, or it may be that analog DCX is just more complicated. It has been demonstrated phenomenologically[19] that the analog and nonanalog data can be understood together provided that the phase of the nonanalog amplitude is adjusted appropriately. In the current approach, the phase of the Δ_{33}-nucleon interaction would be modified by considering two-pion-exchange processes; estimates indicate that this correction to the phase would lead to a destructive interference with the sequential terms at resonance, which could help explain the angular distribution for analog transitions. It would be interesting to see whether currently fashionable meson-exchange models of the nucleon-nucleon interaction would provide the correct magnitude.

In conclusion, we have presented calculations that show that nonanalog double charge exchange for energies from 100 to 300 MeV is qualitatively explained by a simple delta-nucleon interaction (DINT) mechanism. The DINT mechanism describes the angle and energy dependence of the cross sections, whereas the use of realistic wave functions determines the smooth mass dependence. We believe that extensions of the current model in several of the directions discussed would be interesting.

Noted added in proof. The results shown in the text for models I–III correspond to the fixed nucleon approximation. If we make a correction for this by multiplying the external pion legs in Fig. 1 by $m_\pi/E_{\text{c.m.}}$, then the values of $(\Lambda_\pi,\Lambda_\rho)$ become (4.4,5.13), (5.5,6.41), and (5.2,6.07) fm^{-1} for models I–III, respectively, with only very small changes in the results otherwise. We thank M. Burlein for running the calculations.

This work was supported in part by the U.S. Department of Energy and the National Science Foundation.

*Current address: Theoretical Division, Los Alamos National Laboratory, Los Alamos, NM 87545.

†Current address: NORDITA, Blegdamsvej 17, DK-2100 Copenhagen Ø, Denmark.

[1]R. Gilman *et al.*, Phys. Rev. C **32**, 349 (1985).

[2]M. B. Johnson *et al.*, Phys. Rev. Lett. **52**, 593 (1984).

[3]See P. A. Seidl *et al.*, Phys. Rev. C **30**, 973 (1984), and references therein.

[4]A. Wirzba, H. Toki, E. R. Siciliano, M. B. Johnson, and R. Gilman (unpublished).

[5]T. Karapiperis and T. Kobayashi (unpublished).

[6]A. Etchegoyen, W. D. M. Rae, N. S. Godwin, and B. A. Brown, Michigan State Cyclotron Laboratory Report 524, 1985.

[7]B. A. Brown, W. A. Richter, and N. S. Godwin, Phys. Rev. Lett. **45**, 1681 (1980).

[8]S. Cohen and D. Kurath, Nucl. Phys. **73**, 1 (1973).

[9]J. B. McGrory and B. H. Wildenthal, Phys. Rev. C **7**, 974 (1973).

[10]B. H. Wildenthal, *Progress in Particle and Nuclear Physics*, edited by D. H. Wilkinson (Pergamon, Oxford, 1984), Vol. 11, p. 5.

[11]M. Sakakura, A. Arima, and T. Sebe, Phys. Lett. **61B**, 335 (1976).

[12]A. G. M. van Hess and P. W. M. Glaudemans, Z. Phys. A **303**, 276 (1981).

[13]J. E. Koops and P. W. M. Glaudemans, Z. Phys. A **280**, 181 (1977).

[14]See, e.g., R. Gilman, Ph.D. thesis, University of Pennsylvania, 1985; Los Alamos National Laboratory Report LA-10524-T, 1985; or L. C. Bland, in Proceedings of the LAMPF Workshop on Pion Double Charge Exchange, Los Alamos National Laboratory Report LA-10550-C, 1985, p. 245.

[15]K. Holinde, Phys. Rep. **68**, 121 (1981).

[16]J. Speth and M. B. Johnson (unpublished).

[17]G. E. Brown, S. O. Bäckman, E. Oset, and W. Weise, Nucl. Phys. **A286**, 191 (1977).

[18]W. B. Cottingame and D. B. Holtkamp, Phys. Rev. Lett. **45**, 1828 (1980).

[19]S. J. Greene, *et al.*, Phys. Rev. C **25**, 924 (1982); R. Gilman *et al.*, Nucl. Phys. **A432**, 610 (1985); R. Gilman and H. T. Fortune, submitted to Nucl. Phys.